

# Cure Kinetics and Catalyzed Effect of Hydroxyl Group of LC Diglycidyl Ether of Bisphenol-S with Aromatic Diamines

Li Huo,<sup>1,2</sup> Jungang Gao,<sup>1</sup> Xiaona Zhang<sup>1</sup>

<sup>1</sup>College of Chemistry and Environmental Science, Hebei University, Baoding 071002, China

<sup>2</sup>Department of Chemistry, Baoding University, Baoding 071000, China

Received 12 September 2008; accepted 6 March 2009

DOI 10.1002/app.30384

Published online 8 May 2009 in Wiley InterScience (www.interscience.wiley.com).

**ABSTRACT:** The curing reactions of liquid crystalline 4,4'-bis-(2,3-epoxypropyloxy)-sulfonyl-bis(1,4-phenylene) (*p*-BEPSBP) with 4,4'-diaminodiphenylmethane (DDM) and 4,4'-diaminodiphenylsulfone (DDS) were investigated by nonisothermal differential scanning calorimeter (DSC). The relationships of  $E_a$  with the conversion  $\alpha$  in the curing process were determined. The catalyzed activation of hydroxyl group for curing reaction of epoxy resins with amine in DSC experiment was discussed. The results show that these curing reactions can be described by the autocatalytic Šesták-Berggren model. The curing technical temperature and parameters were obtained, and the even reaction orders  $m$ ,  $n$ , and  $\Delta S$  for *p*-BEPSBP/DDM and *p*-BEPSBP/DDS are 0.35, 0.92,  $-81.94$

and 0.13, 1.32,  $-24.45$ , respectively. The hydroxyl group has catalyzed activation for the epoxy-amine curing system in the DSC experiment. The average  $E_a$  of *p*-BEPSBP/DDM is  $67.19 \text{ kJ mol}^{-1}$  and is  $105.55 \text{ kJ mol}^{-1}$  for the *p*-BEPSBP/DDS system, but it is different for the two systems; when benzalcohol as hydroxyl group was added to the curing system, the average  $E_a$  of *p*-BEPSBP/DDM decreases and increases for *p*-BEPSBP/DDS. The crystalline phase had formed in the curing process and was fixed in the system. © 2009 Wiley Periodicals, Inc. *J Appl Polym Sci* 113: 3693–3701, 2009

**Key words:** liquid crystal epoxy resin; curing kinetics; aromatic amine; hydroxyl group

## INTRODUCTION

The curing reactions of epoxy resins with amine are widely used. Many authors have made the theoretical and experimental investigations and given useful information for the curing reaction of epoxy resins and liquid crystalline epoxy resins (LCER) with aromatic diamines.<sup>1–4</sup> Ehlers et al. had calculated the apparent reaction activation energy ( $E_a$ ) of epoxy resins with amine in the solution for different reaction pathways and concluded that hydroxyl groups have a catalyzed activation and can decrease the  $E_a$  for curing reactions of epoxy resins.<sup>5–7</sup> However, the curing mechanisms and catalyzed effect of hydroxyl group are still not completely understood in a practical differential scanning calorimeter (DSC) experiment. It is significant for studying the reaction kinetics and the chemical and physical factors of curing process, because it has not solvent in most practical work.

In this article, the cure kinetics of liquid crystalline diglycidyl ether of bisphenol-S with 4,4'-diaminodi-

phenylmethane (DDM) and 4,4'-diaminodiphenylsulfone (DDS), and the catalyzed activation of hydroxyl groups, were investigated by nonisothermal DSC method. The relationships of apparent  $E_a$  with the conversion  $\alpha$  for the two curing systems were calculated by Ozawa's method.<sup>8</sup> Some kinetic parameters were evaluated by the autocatalytic kinetic model of the Šesták-Berggren (S-B) equation.<sup>9,10</sup> The molecular mechanism of the curing reaction was discussed.

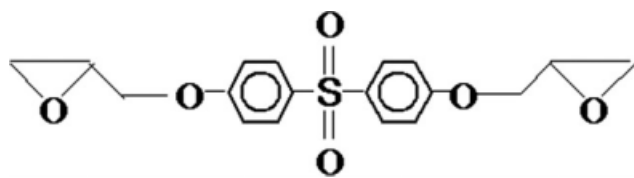
## MATERIALS AND METHODS

### Materials and instrumentation

The 4,4'-bis-(2,3-epoxypropyloxy)-sulfonyl bis(1,4-phenylene) (*p*-BEPSBP) was synthesized from allyl bromide and bisphenol-S according to Ref. 11. Bisphenol-S (10.0 g, 0.04 mol) was dissolved in 80 mL acetone and was introduced in a 250-mL flask; then allyl bromide (8 mL, 0.1 mol),  $\text{K}_2\text{CO}_3$  (13.8 g, 0.1 mol) and cetyltrimethyl ammonium bromide (1.46 g, 0.004 mol) were added to the flask with stirring and refluxed for 24 h. Then the mixture was cooled to room temperature, filtered, and evaporated. The final white solid was recrystallized from ethanol and dried in vacuum. The compound obtained from the above step was dissolved by  $\text{CH}_2\text{Cl}_2$  in a flask, and a calculational amount of

Correspondence to: J. Gao (gaojg@mail.hbu.edu.cn).

Contract grant sponsor: Natural Science Foundation of Hebei Province; contract grant number: B2005000108.



**Scheme 1** The molecular structure of *p*-BEPSBP.

*m*-chloroperbenzoic acid was added and refluxed for 48 h and then filtered off and the filtrate solution was washed successively with 5% NaHSO<sub>3</sub>, 5% NaHCO<sub>3</sub>, and saturated NaCl. The solution was dried over 24 h with MgSO<sub>4</sub> and concentrated under reduced pressure to obtain a white solid; then the white solid (*p*-BEPSBP) was purified by recrystallization from ethyl acetate. The yield is 47% with  $T_m$  at 165°C, and the epoxy value is 0.472 mol/100 g. The epoxy value is smaller than that of theoretical value of 0.552 mol/100 g; this is because some end groups of vinyl have not been oxidized completely. The molecular structure of staples is as shown Scheme 1 and has a smectic texture.

The DDM, DDS, benzalcohol (BA), and other reagents are all analytically pure grades and supplied by the Beijing Chemical Reagent Co. (Beijing, China) in this work.

The phase behavior of the target compounds was characterized by a polarizing optical microscopic (POM; 59XA, Yong-Heng, Shanghai, China). The curing reactions were carried out on a DSC (Diamond, Perkin-Elmer, USA). The DSC instrument was calibrated with high-purity indium. The X-ray diffraction patterns were recorded by monitoring the diffraction angle  $2\theta$  from 0.6° to 45° by using an X-ray diffractometer (XRD; Rigaku-D/max-2500, Germany). The diffractometer was equipped with Cu K $\alpha$  ( $\lambda = 0.1542$  nm) radiation, produced under conditions of 40 kV and 100 mA. FTIR (Bio-Rad FTS-40, USA) was used for infrared analysis. <sup>1</sup>H-NMR (Bruker 400 MHz, Switzerland) spectra were obtained with tetramethylsilane as internal standard.

### Characterization of cured system

The DDM and DDS were used as curing agents for *p*-BEPSBP. The samples of curing reaction were prepared with a stoichiometric ratio of one epoxy group to one N-hydrogen. The *p*-SBPEPB and curing agents were mixed homogeneously and ground into fine powder under an ice bath. About 6 mg samples was placed into an aluminum DSC sample cell and sealed with an aluminum lid and heated from 298 to 523 K under nitrogen flow of 20 mL min<sup>-1</sup>. The dynamic DSC analysis was performed at four heating rates  $\beta$ : 5, 10, 15, 20 K min<sup>-1</sup>, respectively.

The benzalcohol (BA) was added into the mixture of *p*-BEPSBP/DDM or *p*-BEPSBP/DDS in 2% of total weight and marked as *p*-BEPSBP/DDM/BA and *p*-BEPSBP/DDS/BA, respectively. The corresponding experiments were carried out for determining the catalyzed effect of hydroxyl group.

## RESULTS AND DISCUSSION

### Curing reaction mechanism and activation energy

For the nonisothermal curing process, the kinetic parameters can be determined by the isoconversional method of Ozawa.<sup>7,8</sup> Equation (1) is known as Ozawa's equation, which can be used for different conversions  $\alpha$  of the curing process. Thus, for a given  $\alpha$ , the  $E_a$  can be obtained from linear regression.

$$\ln \beta = A' - 1.052 \frac{E_a}{RT} \quad (1)$$

where  $A'$  is the pre-exponential factor of the Arrhenius equation,  $A' = \lg(AE_a/g(\alpha)R) - 3.315$ ,  $g(\alpha) = \int_0^\alpha \frac{d\alpha}{f(\alpha)} = \frac{A}{\beta} \int_0^T \exp(-E_a/RT) dT$ , and  $f(\alpha)$  is a temperature-dependent kinetic model function.

Figure 1 shows the DSC curves of *p*-BEPSBP/DDM and *p*-BEPSBP/DDS cured at four heating rates, respectively. As seen from Figure 1, the two curing systems have all lower eutectic points, and the melting peaks are stronger at a high heating rate. The temperature ranges of curing reaction become broader, and the initial curing temperature,  $T_{ic}$ , the peak temperature,  $T_{pc}$ , and the finishing temperature,  $T_{fc}$ , are all increased as the heating rate increases. Because the different heating rates correspond to the different best curing temperature, the curing technical temperature or information can be obtained from extrapolated plots of  $T$ - $\beta$  curve. These technical temperatures are as follows: for *p*-BEPSBP/DDM, the  $T_{ic}$ ,  $T_{pc}$ , and  $T_{fc}$  are 356.1, 382.2, and 401.4 K, respectively; for *p*-BEPSBP/DDS, the  $T_{ic}$ ,  $T_{pc}$ , and  $T_{fc}$  are 426.4, 442.3, and 476.5 K, respectively.

The relationships of conversion  $\alpha$  vs. dynamic curing temperature  $T$  for *p*-BEPSBP/DDM and *p*-BEPSBP/DDS systems are shown in Figure 2. As seen from Figure 2, at the same conversion  $\alpha$  value, the isoconversion temperature is higher as the heating rate increases. According to  $\alpha$ - $T$  and Ozawa's eq. (1), from the plot of  $\ln \beta$  vs.  $1/T$ , the apparent activation energy  $E_a$  at any conversion  $\alpha$  can be calculated. The linear coefficients of  $\ln \beta$  with  $1/T$  are all included between 0.9952 and 0.9991, and it shows that the two curing systems all well obey Ozawa's kinetics model. The results are shown in Figure 3.

As seen from Figure 3, the  $E_a$  changes at various conversions  $\alpha$  and gradually decreases as the  $\alpha$

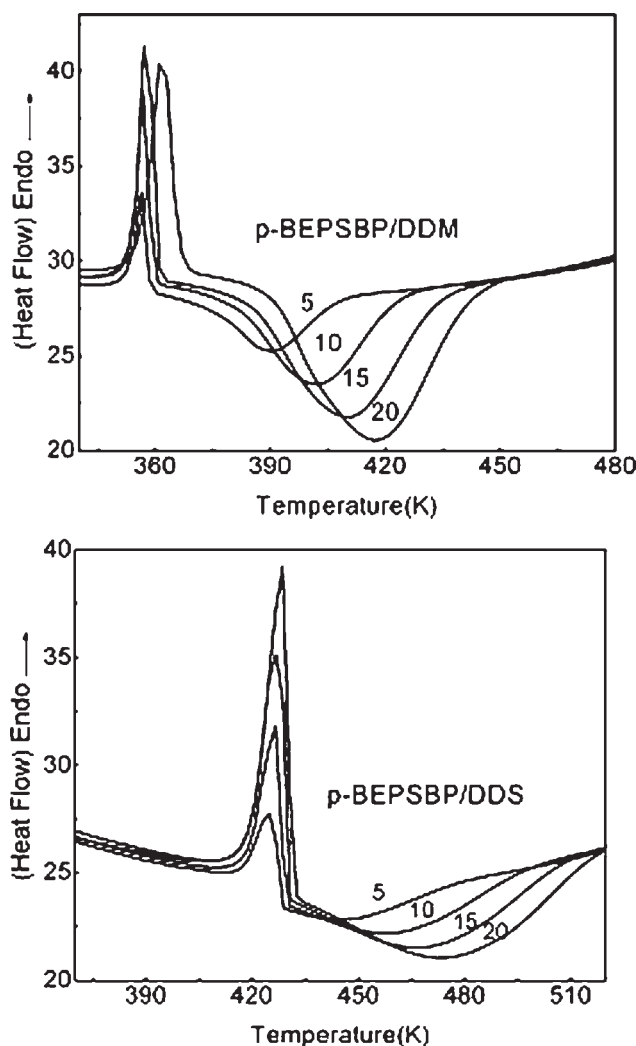


**Figure 1** The cured DSC curves of *p*-BEPSBP/DDM and *p*-BEPSBP/DDS systems at different heating rates.

increases in the curing prophase (0–0.25) besides *p*-BEPSBP/DDM/BA. This result is coincident with conclusions of Rosu et al.<sup>10</sup> They reported that the curing reaction  $E_a$  of diglycidyl ether of 4,4'-bisphenol with sulfanilamide gradually decreased as the  $\alpha$  increased. However, when  $\alpha$  is over 0.25 (for *p*-BEPSBP/DDM is over 0.1),  $E_a$  for these systems only have very little variation or keep constant. The average  $E_a$  is  $67.19 \text{ kJ mol}^{-1}$  for *p*-BEPSBP/DDM and is  $105.55 \text{ kJ mol}^{-1}$  for the *p*-BEPSBP/DDS system. The reaction  $E_a$  is higher,  $10\text{--}20 \text{ kJ mol}^{-1}$ , than that of the reaction of noncrystalline bisphenol-S epoxy resin with DDS and DDM (as we had reported in Refs. 12 and 13 by isothermal DSC); the reason may be that the smectic texture of LC epoxy resins have a higher steric effect to reaction with aromatic diamines because of the higher order.

The mechanism of curing reaction for epoxy resins/amine is complex due to gelation and

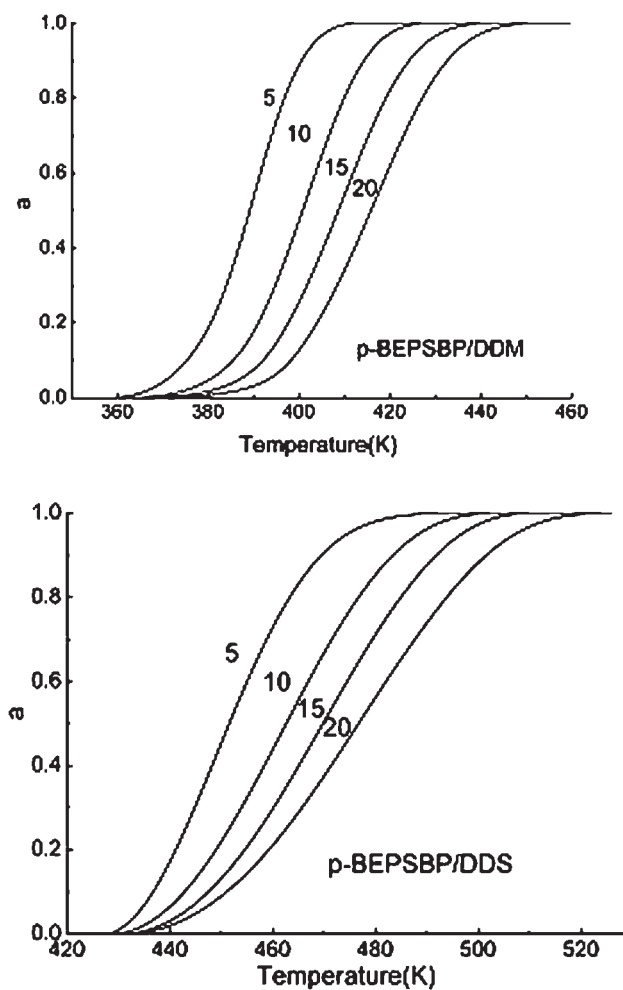


**Figure 2**  $\alpha$  vs.  $T$  curves of *p*-BEPSBP/DDM and *p*-BEPSBP/DDS at different heating rates.

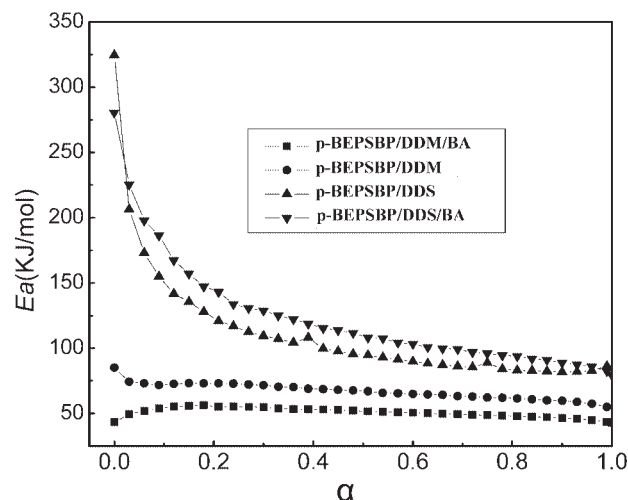
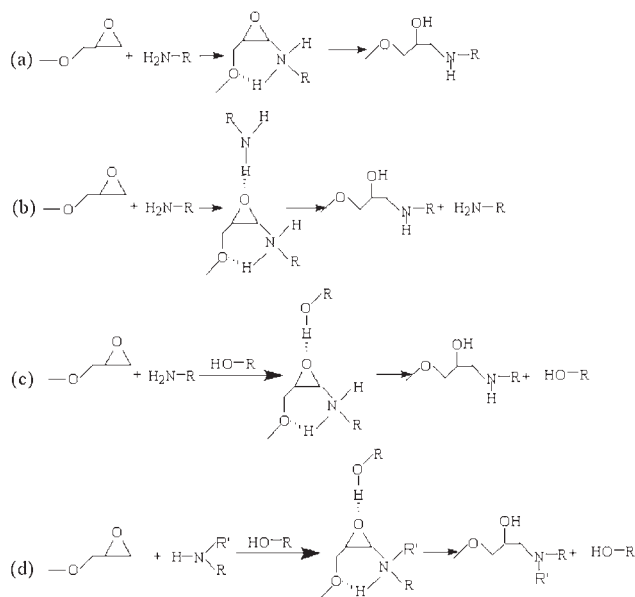


**Figure 3** The relationship of  $E_a$  calculated vs.  $\alpha$  by the Ozawa method for the *p*-BEPSBP/DDM and *p*-BEPSBP/DDS systems.

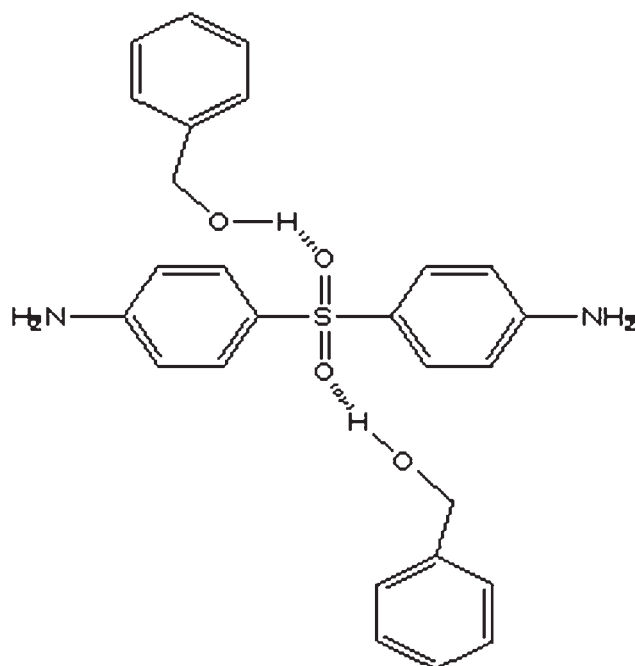


**Scheme 2** Transition states of the reaction pathways. (a) Uncatalyzed, (b) self-promoted, (c) alcohol-catalyzed, (d) second amine.

vittrification in the curing process. For *p*-BEPSBP/DDS, the  $E_a$  is  $324.4 \text{ kJ mol}^{-1}$  in the started stages, which is higher than that of *p*-BEPSBP/DDM ( $85.2 \text{ kJ mol}^{-1}$ ). The curing reaction between the epoxy ring and amine is known as a nucleophilic reaction of opening ring. The reaction rate and  $E_a$  are related to the nucleophilicity of the amine group in the reaction site. The sulfone group in DDS has more electron withdrawing character than the methylene group in DDM and can form a resonance state with two phenyls in DDS. Therefore, the N in DDS has lower nucleophilic ability than that of N in DDM, so *p*-BEPSBP/DDS has higher  $E_a$  than that of *p*-BEPSBP/DDM in the started stages. On the other hand, the effect of molecular mechanism of curing reaction on the curing  $E_a$  is also a primary reason. There are different transition states in the curing reaction of epoxy resins with amines. These transition states are shown in Scheme 2(a), (b), (c), and (d), in which (a) is uncatalyzed, (b) is the self-promoted, and (c) is the hydroxyl catalyzed reaction pathway. According to the conclusion of Ehlers,<sup>6</sup> the reaction (a) of the primary amine with an epoxy ring has a higher steric effect of cyclic transition states than that of secondary amines (b) and a higher reactive  $E_a$ . Because the primary amine is the main body in the initial stage of curing reaction, it has a higher  $E_a$  than that of other stages.

It is noteworthy that a hydroxyl group will be generated in the reaction of epoxy group with amine (Scheme 2). To determine the catalyzed activation of the alcohol-hydroxyl group in the DSC experiment, the corresponding experiments were done in exis-

tence of BA. As seen from Figure 3, the  $E_a$  of the *p*-BEPSBP/DDM/BA system is  $50.61 \text{ kJ mol}^{-1}$ , which is lower than that of the *p*-BEPSBP/DDM system ( $67.19 \text{ kJ mol}^{-1}$ ). The result shows that the alcohol-catalyzed activation is also a key factor and has a lower activation barrier than the other. However, for *p*-BEPSBP/DDS/BA, the  $E_a$  ( $123.40 \text{ kJ mol}^{-1}$ ) is higher than that of *p*-BEPSBP/DDS ( $105.55 \text{ kJ mol}^{-1}$ ). This is because oxygen of sulfonyl in DDS can form a hydrogen bond with the hydroxyl groups of BA (Scheme 3) and enhance the molecular steric hindrance and decrease the nucleophilicity of amine in DDS. The end distances of DDS/BA and DDS were calculated (concluded by Chem3D) ( $0.9548 \text{ nm}$  for DDS/BA) and were shorter than that of DDS (DDS is  $0.9748 \text{ nm}$ ). The hydroxyl bond between DDS and BA could be proved by FTIR or NMR (Fig. 4). As seen from Figure 4, the  $-\text{OH}$  peak of BA is split into three peaks  $\delta$  (ppm) ( $5.19, 5.18, 5.16$ ) in  $^1\text{H-NMR}$  of BA and becomes single and weak ( $\delta = 5.19$ ). The  $\delta = 7.64$  of  $\text{Ar-H}$  for DDS shifts to  $7.49$  in DDS/BA. The hydrogen bonding in DDS/BA was also revealed by FTIR; the absorbing peak of the  $-\text{OH}$  group at  $3400 \text{ cm}^{-1}$  disappeared in the FTIR spectra of DDS/BA but are not changed in DDM/BA. These results all illuminated that the hydrogen bond had formed between the sulfonyl group of DDS and BA. However, the hydrogen bond has a dependence on temperature,<sup>14,15</sup> which will be weakened or disappear as the temperature increases. Therefore, it has a higher  $E_a$  at the start of the curing reaction but decreased quickly as temperature



**Scheme 3** Hydrogen bond structure of *p*-BEPSBP/DDS/BA.

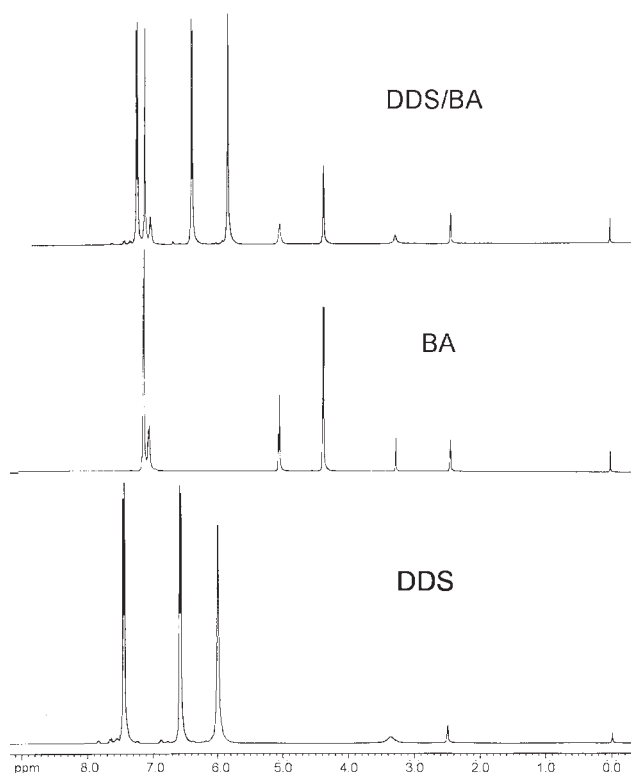


Figure 4  $^1\text{H-NMR}$  spectra of DDS/BA, DDS, and BA.

increases in nonthermal DSC for the *p*-BEPSBP/DDS/BA system.

The results show that hydroxyl groups can accelerate the curing reaction and decrease  $E_a$  for *p*-BEPSBP/DDM. However, for *p*-BEPSBP/DDS, the  $E_a$  will be increased after adding BA, which is also one causation that *p*-BEPSBP/DDS has a higher  $E_a$  than *p*-BEPSBP/DDM because the hydroxyl group is also generated in the reaction of epoxy group with amine and the hydrogen bond may be formed in the *p*-BEPSBP/DDS system.

#### Cure kinetics of *p*-BEPSBP/DDM and *p*-BEPSBP/DDS

The reaction rate ( $d\alpha/dt$ ) in the kinetic analysis can be described as follows:

$$\frac{d\alpha}{dt} = k(T)f(\alpha) \quad (2)$$

where  $f(\alpha)$  is a dependent kinetic model function, and  $k(T)$  is a temperature-dependent reaction rate constant and follows an Arrhenius equation:

$$k(T) = A \exp\left(\frac{-E_a}{RT}\right) \quad (3)$$

Considering that eq. (3) is valid for dynamic curing reaction and  $d\alpha/dt = \beta(d\alpha/dT)$ , where  $\beta = dT/dt$

is the heating rate ( $\text{K min}^{-1}$ ), eq. (2) can be modified as follows:

$$\beta \frac{d\alpha}{dT} = A \cdot e^{(-E_a/RT)} \cdot f(\alpha) \quad (4)$$

where  $T$  is the temperature (K),  $A$  is the pre-exponential factor, and  $E_a$  is the apparent activation energy.

Once  $E_a$  has been determined, the most suitable kinetic model can be evaluated with the functions  $y(\alpha)$  and  $z(\alpha)$  according eqs. (5) and (6)<sup>9,10</sup>:

$$y(\alpha) = \frac{d\alpha}{dt} \cdot \exp(x) \quad (5)$$

$$z(\alpha) = \pi(x) \cdot \left(\frac{d\alpha}{dt}\right) \cdot \frac{T}{\beta} \quad (6)$$

where  $x$  is the reduced activation energy ( $E_a/RT$ ),  $\beta$  represents the heating rate ( $\text{K min}^{-1}$ ),  $T$  is the absolute temperature (K), and  $\pi(x)$  denotes an approximation of the temperature integral, which is

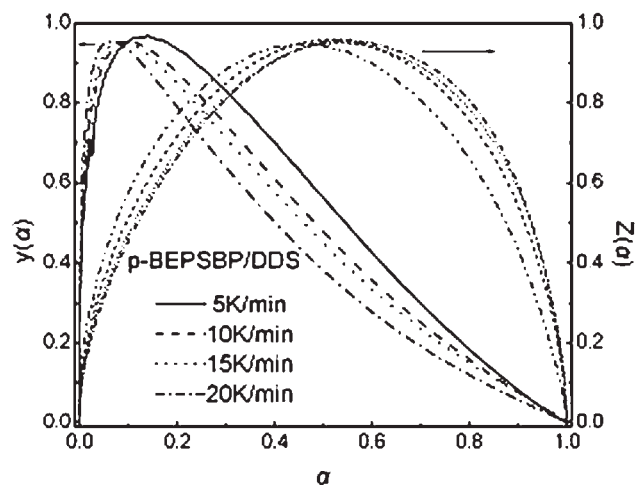
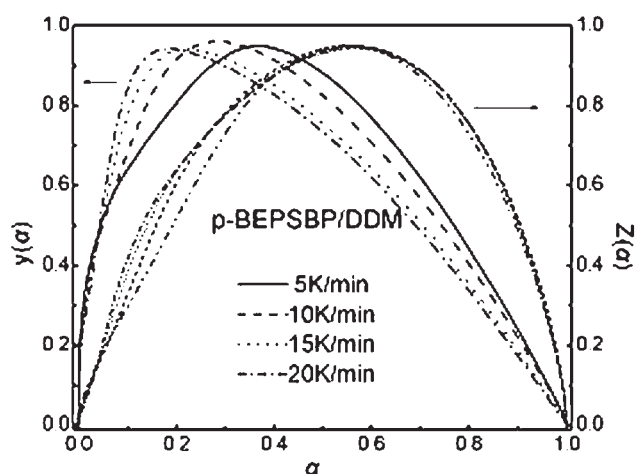


Figure 5 Variation of normalized  $y(\alpha)$  and  $z(\alpha)$  function vs.  $\alpha$  for the *p*-BEPSBP/DDM and *p*-BEPSBP/DDS systems.

**TABLE I**  
The Values of  $\alpha_p$ ,  $\alpha_M$ ,  $\alpha_p^\infty$  Obtained from DSC Data for the Curing System

Sample	Heating rate (K min <sup>-1</sup> )	$\alpha_p$	$\alpha_M$	$\alpha_p^\infty$
BEPSBP/DDM	5	0.536	0.358	0.549
	10	0.532	0.294	0.564
	15	0.540	0.220	0.562
	20	0.544	0.205	0.554
<i>p</i> -BEPSBP/DDM/BA	5	0.439	0.297	0.474
	10	0.439	0.177	0.469
	15	0.461	0.163	0.494
	20	0.462	0.138	0.493
<i>p</i> -BEPSBP/DDS	5	0.402	0.109	0.450
	10	0.480	0.096	0.515
	15	0.486	0.086	0.534
	20	0.501	0.066	0.545
<i>p</i> -BEPSBP/DDS/BA	5	0.451	0.166	0.468
	10	0.500	0.102	0.590
	15	0.461	0.064	0.564
	20	0.710	0.056	0.720

approximated by using the fourth rational expression:

$$\pi(x) = \frac{x^3 + 18x^2 + 88x + 96}{x^4 + 20x^3 + 120x^2 + 240x + 120} \quad (7)$$

For practical reasons, the  $y(\alpha)$  and  $z(\alpha)$  functions are normalized within the (0, 1) range. The maximum  $\alpha_M$  of the  $y(\alpha)$  function and  $\alpha_p^\infty$  of the  $z(\alpha)$  function help us to determine the most suitable kinetic model characterizing the curing process.

Figure 5 shows the variation of  $y(\alpha)$  and  $z(\alpha)$  values with conversion  $\alpha$  for *p*-BEPSBP/DDM and *p*-BEPSBP/DDS, respectively. Table I lists the values of  $\alpha_M$  and  $\alpha_p^\infty$ , together with  $\alpha_p$ , taken as the conversion maximum at the DSC peak.

As can be noted from Table I, the  $\alpha_M$  values are lower than the  $\alpha_p$  values and  $\alpha_M \neq 0$ , so the curing process of two curing systems can be described by using a two-parameter autocatalytic model of the Šesták–Berggren (S–B) eq. (8)<sup>9,10</sup>:

$$f(\alpha) = k\alpha^m(1 - \alpha)^n \quad (8)$$

$$\ln[(d\alpha/dt) \cdot e^x] = \ln A - n \ln[\alpha^p \cdot (1 - \alpha)] \quad (9)$$

where  $k$  is the rate constant,  $A$  presents the pre-exponential factor,  $m$  and  $n$  are the reaction orders, and  $m$  is a reaction order when  $\alpha = 0$ , so  $n$  is a primary order in the reaction process (when  $\alpha$  is not zero).

Table II lists the kinetic parameters ( $m$ ,  $n$ ,  $\ln A$ , and  $E_a$ ), which are experimentally obtained according to the proposed S–B kinetic model. The kinetic parameters  $n$  and  $\ln A$  are obtained by the slope and intercept of the linear dependence  $\ln[(d\alpha/dt)e^x]$  vs.  $\ln[\alpha_p(1 - \alpha)]$  according to eq. (9), where  $m = pn$  and  $p = \alpha_M/(1 - \alpha_M)$ . The linear coefficients of kinetic parameters in Table II are all between 0.9923 and 0.9992, which further indicates that the two curing systems all obey the S–B model. As it is shown in Table II, for *p*-BEPSBP/DDM and *p*-BEPSBP/DDS, the  $m$  are all decreased when BA is added; that is to say, the effect of adding BA is the same for the two systems at  $\alpha = 0$ . However, the value of  $n$  becomes larger for the *p*-BEPSBP/DDM system after adding BA, and the  $n$  of *p*-BEPSBP/DDS/BA is smaller than that of *p*-BEPSBP/DDS. The results show the reaction rate of *p*-BEPSBP/DDM is increased and is decreased for *p*-BEPSBP/DDS after the addition of BA, which indicates that the effect of BA and hydroxyl group on the *p*-BEPSBP/DDM and *p*-BEPSBP/DDS is different. The values of  $\ln A$  have a

**TABLE II**  
Apparent Kinetic Parameters Evaluated for Nonisothermal Curing Systems

Sample	Heating rate (K min <sup>-1</sup> )	$E_a$ (kJ mol <sup>-1</sup> )	$\ln A$	Mean	$m$	Mean	$n$	Mean	$\Delta S$ (J K <sup>-1</sup> mol <sup>-1</sup> )	Mean
BEPSBP/DDM	5	67.191	20.21	19.77	0.53	0.35	0.95	0.92	-79.11	-81.94
	10		19.94		0.36		0.88		-81.61	
	15		19.80		0.26		0.92		-82.94	
	20		19.68		0.24		0.95		-84.09	
BEPSBP/DDM/BA	5	50.610	15.50	15.20	0.43	0.25	1.02	1.00	-117.90	-120.78
	10		15.19		0.21		0.98		-120.82	
	15		15.10		0.18		0.95		-121.75	
	20		15.01		0.17		1.04		-122.67	
<i>p</i> -BEPSBP/DDS	5	105.50	27.24	26.94	0.18	0.13	1.20	1.32	-21.85	-24.45
	10		27.00		0.14		1.31		-24.08	
	15		26.88		0.12		1.29		-25.20	
	20		26.72		0.10		1.47		-26.67	
<i>p</i> -BEPSBP/DDS/BA	5	123.40	36.19	35.82	0.18	0.10	0.90	1.00	53.41	50.11
	10		35.88		0.11		0.98		50.68	
	15		35.79		0.068		1.18		49.83	
	20		35.42		0.055		0.93		46.53	

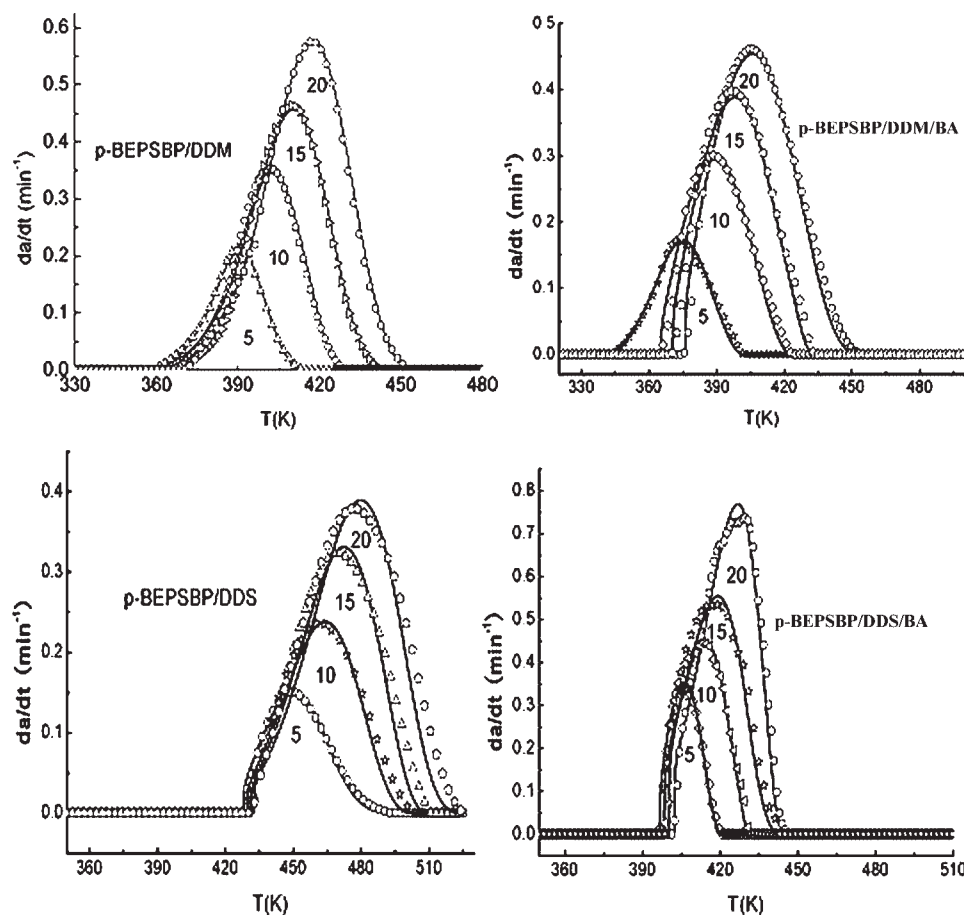


**Figure 6** Experimental (symbols) and calculated (full lines) DSC curves for the curing systems of *p*-BEPSBP/DDM, *p*-BEPSBP/DDM/BA, *p*-BEPSBP/DDS, and *p*-BEPSBP/DDS/BA.

certain difference for the two systems (Table II).  $A$  is related to the activation entropy  $\Delta S$ . The  $\Delta S$  of the two curing systems were evaluated using eq. (10):

$$A = \frac{KT_p}{h} \cdot \exp\left(\frac{\Delta S}{R}\right) \quad (10)$$

where  $K$  is the Boltzmann constant,  $h$  is the Planck constant, and  $T_p$  is the peak temperature of DSC curves.

The  $\Delta S$  that obtained from eq. (10) is listed in Table II. The negative values of  $\Delta S$  indicate that the activated complexes have a more ordered structure than the reactants for the *p*-BEPSBP/DDM system, but the positive values of  $\Delta S$  for the *p*-BEPSBP/DDS system show that the transition states have a lower order than reactants,<sup>16,17</sup> which is coincident with the description of hydrogen bond.

The experimental curves (symbols) of  $d\alpha/dt$  vs.  $T$  and theoretical curves (full lines) calculated using the kinetic parameters to each heating rate (see Table II) are compared in Figure 6. A good coincidence can be seen between the theoretical curves and those experimentally determined for *p*-BEPSBP/DDM, *p*-BEPSBP/DDM/BA, and *p*-BEPSBP/DDS/

BA. This means that the two-parameter S-B ( $m, n$ ) model can give a good description for the curing process of *p*-BEPSBP/DDM. However, for *p*-BEPSBP/DDS, some deviation appears in the last stage. This is because the DDS has a higher melting point and a larger polarity than that of DDM, so that *p*-BEPSBP/DDS system has larger viscosity than *p*-BEPSBP/DDM and *p*-BEPSBP/DDS/BA (the addition of small molecule BA can decrease the viscosity of reaction system), and decreased mobility of reactive groups. In this condition, the rate of conversion is controlled by diffusion rather than by kinetic factors. Simultaneously, we may see that the S-B ( $m, n$ ) model is well fit to describe the hydroxyl group catalyzed curing system and the situation of lower heating rate ( $\leq 15 \text{ K min}^{-1}$ ). It can find that the curing temperature of systems catalyzed by the hydroxyl group are all lower than that of uncatalyzed curing systems at the same conversion  $\alpha$ .

#### Mechanical loss and textures of curing products

Because the glass transition temperature ( $T_g$ ) can be used effectively to monitor the molecular motion

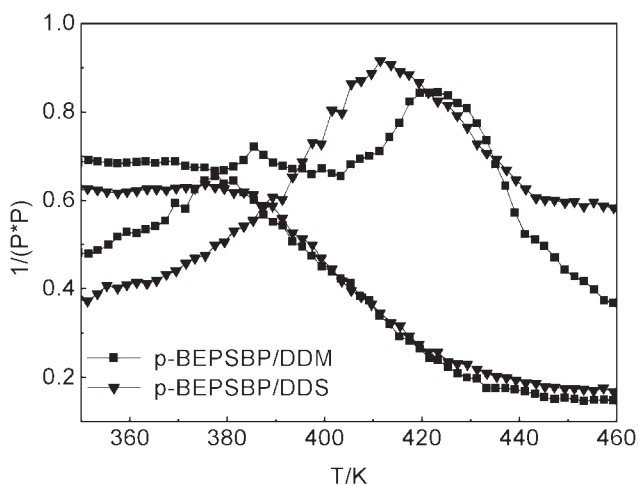


**Figure 7** Dynamic mechanical graphs of the *p*-BEPSBP/DDM and *p*-BEPSBP/DDS.

and curing reaction, the torsional braid analysis (TBA) method can be used to determine the  $T_g$  of the thermosetting system, and it is particularly useful at high conversion and after vitrification because of the nonlinearity of  $T_g$  vs. conversion  $\alpha$ .<sup>18</sup> Generally, the higher mechanical loss peak temperature ( $T_p$ ), the higher the  $T_g$  is, which depends on the curing conditions, such as amount of cross-linked agent, curing temperature, and time. The curing conditions, the peak temperature  $T_p$ , and  $T_g$  of the samples can be changed so that  $T_g$  is used directly as a parameter in the analysis of reaction kinetic models, which can

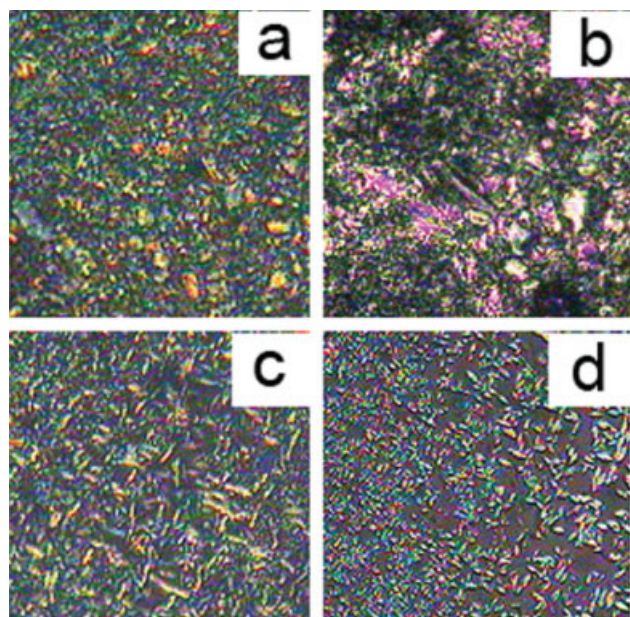


**Figure 8** POM photographs ( $\times 400$ ) of curing systems; *p*-BEPSBP/DDM: (a) 383 K 5 min; (b) 383 K 15 min; *p*-BEPSBP/DDS: (c) 423 K 5 min; (d) 423 K 15 min. [Color figure can be viewed in the online issue, which is available at [www.interscience.wiley.com](http://www.interscience.wiley.com).]

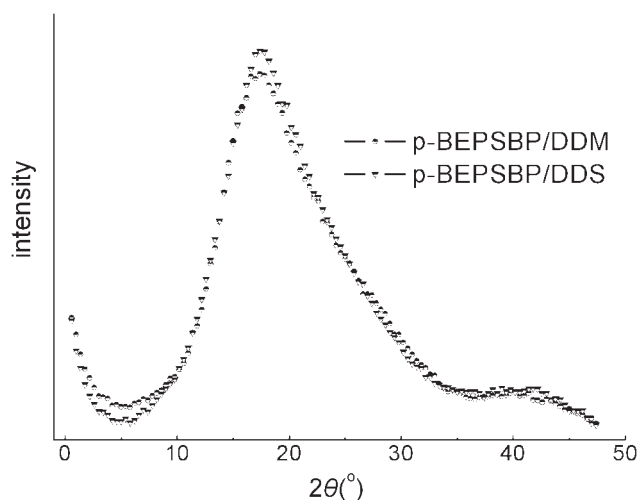


**Figure 9** The XRD spectra of cured samples for *p*-BEPSBP/DDM and *p*-BEPSBP/DDS.

be determined by TBA.<sup>19</sup> Figure 7 is the TBA graph of cured systems. As seen from Figure 7, we can obtain the  $T_p$  of *p*-BEPSBP/DDM at 420 K, and 411 K for *p*-BEPSBP/DDS.

POM and XRD were used to monitor the texture of curing samples. The POM observations of the curing reaction were held at 383 K for *p*-BEPSBP/DDM and at 423 K for *p*-BEPSBP/DDS, respectively, then subsequently quenched rapidly to room temperature and observed by POM (shown in Fig. 8). As seen from Figure 8, the brightness spots of cosh shape increased more and more in the curing process, showing that the nematic texture was formed. Figure 9 is XRD curves of cured samples. The curves show only a diffraction peak at  $2\theta = 20^\circ$  for the two curing systems and belong to nematic texture.<sup>20</sup> This is because the LCER molecules have a tendency of self-conglomeration, and the orderly structure had been fixed in the system. The reason of formed nematic texture is that the reaction of LCER molecules with aromatic diamine increases the ratio of length with the radius of curing molecules.

## CONCLUSIONS

1. The nonisothermal curing kinetics of *p*-BEPSBP/DDM and *p*-BEPSBP/DDS all can be described by the Ozawa equation and two-parameter autocatalytic kinetic model of Šesták-Berggren. The even apparent activation energy  $E_a$  of *p*-BEPSBP/DDS is  $105.55 \text{ kJ mol}^{-1}$  and is higher than that of *p*-BEPSBP/DDM ( $67.19 \text{ kJ mol}^{-1}$ ).
2. The even reaction orders  $m$ ,  $n$ , and  $\Delta S$  for *p*-BEPSBP/DDM and *p*-BEPSBP/DDS are 0.35, 0.92,  $-81.94$  and 0.13, 1.32, 24.60, respectively.
3. The hydroxyl group has catalyzed activation and can decrease the  $E_a$  for the epoxy-amine curing



system in the DSC experiment, but it is adverse for the system of DDS as a curing reagent, because a hydrogen bond was formed between molecules of DDS and the hydroxyl group.

## References

1. Amendola, E.; Carfagna, C.; Giamberini, M.; Pisaniello, G. *Macromol Chem Phys* 1995, 196, 1577.
2. Liu, G. D.; Gao, J. G.; Song, L. L.; Hou, W. J.; Zang, L. C. *Macromol Chem Phys* 2006, 207, 2222.
3. Lee, J. Y.; Jang, J.; Hwang, S. S.; Hong, S. M.; Kim, K. U. *Polymer* 1998, 39, 6121.
4. Castell, P.; Serra, A.; Calia, M. J. *Polym Sci Part A: Polym Chem* 2003, 41, 1536.
5. Sbirrazzuoli, N.; Vyazovkin, S.; Mititelu, A.; Sladic, C.; Vincen, L. *Chem Phys* 2003, 204, 815.
6. Ehers, J. E.; Rondan, N. G.; Huynh, L. K.; Pham, H.; Marks, M.; Truong, T. N. *Macromolecules* 2007, 40, 4370.
7. Sbirrazzuoli, N.; Mititelu, M. A.; Vincent, L.; Alzina, C. *Thermochim Acta* 2006, 447, 167.
8. Ozawa, T. *J Therm Anal* 1979, 2, 301.
9. Šesták, J.; Berggren, G. *Thermochim Acta* 1971, 3, 1.
10. Rosu, D.; Mititelu, A.; Cascaval, C. N. *Polym Test* 2004, 23, 209.
11. Huo, L.; Gao, J. G.; Du, Y. G.; Cai, Z. H. *J Appl Polym Sci* 2008, 110, 3671.
12. Li, Y. F.; Shen, S. G.; Liu, Y. F.; Gao, J. G. *J Appl Polym Sci* 1999, 73, 1799.
13. Gao, J. G.; Li, Y. F. *Polym Int* 2000, 49, 1590.
14. Dormidontova, E.; Brinke, G. *Macromolecules* 1998, 31, 2649.
15. Wei, Q.; Cao, H.; Zhang, L.; Yuan, X.; Yang, H.; Wang, Y. *Spectrosc Spect Anal* 2008, 28, 1522 (in Chinese).
16. Si, A.; Majid, K. *Thermochim Acta* 1998, 317, 183.
17. Nair, M. K. M.; Radhakrishnan, P. K. *Thermochim Acta* 1997, 292, 115.
18. Venditti, R. A.; Gillham, J. K. *J Appl Polym Sci* 1997, 64, 3.
19. Gillham, J. K. *Polym Int* 1997, 44, 262.
20. Zhou, Q. F.; Wang, X. J. *Liquid Crystal Polymers*; Science Press: Beijing, 1999; pp 74–108.